Comput Visual Sci (2010) 13:17–28
DOI 10.1007/s00791-008-0122-0

REGULAR ARTICLE

An Eulerian approach to transport and diffusion on evolving implicit surfaces

G. Dziuk · C. M. Elliott

Received: 10 May 2007 / Accepted: 28 January 2008 / Published online: 24 July 2008

Abstract In this article we define a level set method for a scalar conservation law with a diffusive flux on an evolving hypersurface $\Gamma(t)$ contained in a domain $\Omega \subset \mathbb{R}^{n+1}$. The partial differential equation is solved on all level set surfaces of a prescribed time dependent function Φ whose zero level set is $\Gamma(t)$. The key idea lies in formulating an appropriate weak form of the conservation law with respect to time and space. A major advantage of this approach is that it avoids the numerical evaluation of curvature. The resulting equation is then solved in one dimension higher but can be solved on a fixed grid. In particular we formulate an Eulerian transport and diffusion equation on evolving implicit surfaces. Using Eulerian surface gradients to define weak forms of elliptic operators naturally generates weak formulations of elliptic and parabolic equations. The finite element method is applied to the weak form of the conservation equation yielding an Eulerian Evolving Surface Finite Element Method. The computation of the mass and element stiffness matrices, depending only on the gradient of the level set function, are simple and straightforward. Numerical experiments are described which indicate the power of the method. We describe how this framework may be employed in applications.

Communicated by M. Rumpf.

G. Dziuk (✉)
Abteilung für Angewandte Mathematik, University of Freiburg,
Hermann-Herder-Straße 10, 79104 Freiburg i. Br., Germany
e-mail: gerd.dziuk@mathematik.uni-freiburg.de

C. M. Elliott
Mathematics Institute, University of Warwick,
Coventry CV4 7AL, UK
e-mail: C.M.Elliott@warwick.ac.uk

1 Introduction

Partial differential equations on evolving curves and surfaces occur in many applications. In [1] we introduced the evolving surface finite element method (ESFEM) for the numerical solution of diffusion equations on prescribed moving hypersurfaces $\Gamma(t) \subset \mathbb{R}^{n+1}$. The method relies on formulating an appropriate weak form of the conservation law with respect to time and space and on approximating the partial differential equation on a triangulated surface ($n = 2$) or polygonal curve ($n = 1$) which interpolates $\Gamma(t)$, [2].

In this paper, we extend this approach to the formulation and approximation of transport and diffusion of a material quantity on an evolving surface in $\mathbb{R}^{n+1}$ ($n = 1, 2$) to implicitly defined evolving surfaces.The evolving surface is just one level set of a prescribed function and the partial differential equation and its solution are extended to a neighbourhood of the surface. (See [3] where we treated parabolic equations on implicit stationary surfaces.) This neighbourhood is then discretized on a finite element grid which is independent of the surface yielding an Eulerian ESFEM. We have in mind the solution of partial differential equations on surfaces with complex morphology for which the parametric approach may not be or is not adequate. We can treat the case of a surface which not only evolves in the normal direction but also has a tangential velocity associated with the motion of surface material points which advect quantities such as heat or mass. For our purposes here we assume that the surface evolution is prescribed.

In a forthcoming paper, [4], we show that it is sufficient to take the computational domain to be an h-narrow band.

A general framework for formulating partial differential equations on implicit surfaces was proposed by the authors of [5,6]. They considered time dependent second order linear and nonlinear diffusion equations in the context of finite

difference approximations on rectangular grids independent of the surfaces. In [7,8] the authors presented finite difference methods for fourth order parabolic equations on implicit surfaces. A finite element approximation of elliptic equations on implicit surfaces is presented in [9]. Level set methods for solving partial differential equations on evolving surfaces have been proposed in [10,11].

1.1 The advection diffusion equation

Conservation of a scalar quantity u with a diffusive flux on an evolving hypersurface $\Gamma(t)$ leads to the diffusion equation

$$u_t + V\frac{\partial u}{\partial \nu} + \nabla_\Gamma \cdot (u v_S) - VHu - \nabla_\Gamma \cdot (\mathcal{A}\nabla_\Gamma u) = 0 \qquad (1.1)$$

where ν, V, H and v_S are the normal, normal velocity, mean curvature and advective tangential velocity. This equation may be also written as

$$\dot{u} + u\,\nabla_\Gamma \cdot v - \nabla_\Gamma \cdot (\mathcal{A}\nabla_\Gamma u) = 0 \qquad (1.2)$$

on $\Gamma(t)$. Here $\dot{u}$ denotes the covariant or advective surface material derivative, $v = V\nu + v_S$ is the prescribed velocity of the surface and ∇_Γ is the tangential surface gradient. We assume that $\partial\Gamma(t)$ is empty and so the equation does not need a boundary condition. It is this form of the equation which provides the weak formulation underlying our methods.

1.2 Applications

Such a problem arises, for example, when modeling the transport of an insoluble surfactant on the interface between two fluids, [12,13]. Here one views the velocity of the surface as being the fluid velocity and hence the surfactant is transported by advection via the tangential fluid velocity (and hence the tangential surface velocity) as well by diffusion within the surface. The evolution of the surface itself in the normal direction is then given by the normal component of the fluid velocity.

Diffusion induced grain boundary motion, [14–17], has the feature of coupling forced mean curvature flow for the motion of a grain boundary with a diffusion equation for a concentration of mass in the grain boundary. In this case there is no material tangential velocity of the grain boundary so it is sufficient to consider the surface velocity as being in the normal direction.

Another example is pattern formation on the surfaces of growing organisms modelled by reaction diffusion equations, [18]. Possible applications in image processing are suggested by the article [19].

1.3 Outline of paper

The layout of the paper is as follows. We begin in Sect. 2 by defining notation and essential concepts from elementary differential geometry necessary to describe the problem and numerical method. The equations presented above are justified in Sect. 3. The weak form of the equations is derived in Sect. 4 and the well posedness of the initial boundary value problem is established. In Sect. 5 the finite element method is defined and some preliminary approximations results are shown. Implementation issues are discussed in Sect. 6 and the results of numerical experiments are presented.

2 Basic notation and surface derivatives

2.1 Notation

For each $t \in [0,T]$, $T > 0$, let $\Gamma(t)$ be a compact smooth orientable hypersurface without boundary in $\mathbb{R}^{n+1}$ which has a representation defined by a smooth level set function $\Phi = \Phi(x,t)$, $x \in \mathbb{R}^{n+1}$, $t \in [0,T]$ so that

$$\Gamma(t) = \{x \in \Omega : \Phi(x,t) = 0\}$$

where Ω is a bounded domain in $\mathbb{R}^{n+1}$ with Lipschitz boundary $\partial\Omega$. We assume that Φ satisfies the non-degeneracy condition

$$\nabla\Phi \neq 0 \quad \text{in} \quad \Omega \times (0,T). \qquad (2.1)$$

We assume that $\partial\Omega \cap \Gamma(t)$ is empty and set $\nu_{\partial\Omega}$ to be the unit outward pointing normal to $\partial\Omega$. We set $\Omega_T = \Omega \times (0,T)$. In particular we suppose that for some $k \geq 3$ and some $0 < \alpha < 1$

$$\Phi \in C^1([0,T], C^{k,\alpha}(\overline{\Omega})).$$

The orientation of $\Gamma(t)$ is set by taking the normal ν to Γ to be in the direction of increasing Φ. Hence, we define a normal vector field by

$$\nu(x,t) = \frac{\nabla\Phi(x,t)}{|\nabla\Phi(x,t)|}$$

so that the normal ν_Γ to $\Gamma(t)$ is equal to $\nu|_{\Gamma(t)}$ and the normal velocity V of Γ is given by

$$V(x,t) = -\frac{\Phi_t(x,t)}{|\nabla\Phi(x,t)|}.$$

Observe that a possible choice for Φ is the signed distance function $d(x,t)$ to $\Gamma(t)$ and in that case $|\nabla\Phi| = |\nabla d| = 1$ on Ω_T.

The existence of T and Ω and Φ for $t \in [0,T]$ such that the above holds is a consequence of the smoothness of $\Gamma(t)$ in space and time.

Remark 1 The above description of $\Gamma(t)$ relies solely on the normal velocity V. We return to this in Sect. 2.2.

We define the projection

$$\mathcal{P}_\Phi = I - \nu \otimes \nu, \quad (\mathcal{P}_\Phi)_{ij} = \delta_{ij} - \nu_i \nu_j. \tag{2.2}$$

$(i, j = 1, \ldots, n+1)$ so that $\mathcal{P}_\Phi \nu = 0$. For any function η on Ω we define its Eulerian surface gradient by

$$\nabla_\Phi \eta = \nabla \eta - \nabla \eta \cdot \nu \, \nu = \mathcal{P}_\Phi \nabla \eta$$

where, for x and y in $\mathbb{R}^{n+1}$, $x \cdot y$ denotes the usual scalar product and $\nabla \eta$ denotes the usual gradient on $\mathbb{R}^{n+1}$. Note that $\nabla_\Phi \eta \cdot \nu = 0$ and $\nabla_\Gamma \eta = \nabla_\Phi \eta|_\Gamma$ only depends on the values of η restricted to Γ and is the usual tangential (surface) gradient on Γ.

The Eulerian mean curvature is defined in the usual level set way by

$$H_\Phi = -\nabla \cdot \nu = -\nabla \cdot \frac{\nabla \Phi}{|\nabla \Phi|}.$$

Eulerian surface elliptic operators can then be defined in a natural way, for example the Eulerian Laplace–Beltrami operator is defined by

$$\Delta_\Phi \eta = \nabla_\Phi \cdot \nabla_\Phi \eta.$$

We recall the *coarea formula*

Lemma 1 (Coarea formula) *Let for each $t \in [0, T]$, $\Phi(\cdot, t) : \overline{\Omega} \to \mathbb{R}$ be Lipschitz continuous and assume that for for each $r \in (\inf_\Omega \Phi, \sup_\Omega \Phi)$ the level set $\Gamma_r := \{x \in \overline{\Omega} : \Phi(x, \cdot) = r\}$ is a smooth n-dimensional hypersurface in $\mathbb{R}^{n+1}$. Suppose $\eta : \overline{\Omega} \to \mathbb{R}$ is continuous and integrable. Then*

$$\int_{\inf_\Omega \Phi}^{\sup_\Omega \Phi} \left(\int_{\Gamma_r} \eta \right) dr = \int_\Omega \eta |\nabla \Phi|. \tag{2.3}$$

The Eulerian formula for integration by parts over level surfaces is given by the following Lemma.

Lemma 2 (Eulerian integration by parts) *Assume that the following quantities exist. For a scalar function η and a vector field $\mathcal{Q}$ we have*

$$\int_\Omega \nabla_\Phi \eta |\nabla \Phi| = -\int_\Omega \eta H_\Phi \nu |\nabla \Phi| + \int_{\partial\Omega} \eta (\nu_{\partial\Omega} - \nu \cdot \nu_{\partial\Omega} \, \nu) |\nabla \Phi|, \tag{2.4}$$

$$\int_\Omega \nabla_\Phi \cdot \mathcal{Q} |\nabla \Phi| = -\int_\Omega H_\Phi \mathcal{Q} \cdot \nu |\nabla \Phi| + \int_{\partial\Omega} \mathcal{Q} \cdot (\nu_{\partial\Omega} - \nu \cdot \nu_{\partial\Omega} \nu) |\nabla \Phi|, \tag{2.5}$$

$$\int_\Omega \nabla_\Phi \cdot \mathcal{Q} \eta |\nabla \Phi| + \int_\Omega \mathcal{Q} \cdot \nabla_\Phi \eta |\nabla \Phi| = -\int_\Omega \mathcal{Q} \cdot \nu \eta H_\Phi |\nabla \Phi| + \int_{\partial\Omega} \mathcal{Q} \cdot (\nu_{\partial\Omega} - \nu \cdot \nu_{\partial\Omega} \nu) \eta |\nabla \Phi|. \tag{2.6}$$

Proof We employ the notation $\partial_i = \frac{\partial}{\partial x_i}$ and $\partial_{ij} = \frac{\partial^2}{\partial x_i \partial x_j}$. Elementary calculations yield

$$\begin{aligned} \partial_i |\nabla \Phi| &= \nu_k \partial_{ik} \Phi = (D^2 \Phi \, \nu)_i, \\ |\nabla \Phi| \partial_j \nu_k &= \partial_{jk} \Phi - \nu_k (D^2 \Phi \, \nu)_j, \\ |\nabla \Phi| H_\Phi &= -Tr(D^2 \Phi) + \nu \cdot D^2 \Phi \, \nu, \end{aligned}$$

where $D^2 \Phi$ is the Hessian matrix of second derivatives, $Tr(\cdot)$ is the trace of a matrix and we employ the summation convention for repeated indices. Using the definition of ∇_Φ we find that the left-hand side in (2.4) is

$$\text{LHS} := \int_\Omega \nabla_\Phi \eta |\nabla \Phi| = \int_\Omega |\nabla \Phi| (\nabla \eta - \nu \cdot \nabla \eta \nu)$$

and then we employ the standard integration formula on Ω. It follows that

$$\begin{aligned} (\text{LHS})_i &= -\int_\Omega \eta \partial_i |\nabla \Phi| + \int_\Omega \eta \partial_m (\nu_i \nu_m |\nabla \Phi|) \\ &\quad + \int_{\partial\Omega} \eta |\nabla \Phi| ((\nu_{\partial\Omega})_i - \nu_i (\nu \cdot \nu_{\partial\Omega})) \\ &= I + II + III. \end{aligned}$$

Straightforward calculations yield

$$II = \int_\Omega \eta (\nu_i Tr(D^2 \Phi) + (D^2 \Phi \nu)_i - \nu \cdot D^2 \Phi \nu \nu_i).$$

Combining I and II using the formula for H_Φ gives the desired result. □

Remark 2 The boundary terms in the integration by parts formulae disappear when $\nu = \nu_{\partial\Omega}$.

2.2 The material derivative and Leibniz formulae

Let $v : \Omega_T \to \mathbb{R}^{n+1}$ be a prescribed velocity field which has the decomposition

$$v = V \nu + v_\mathcal{S}$$

where

$$V = v \cdot \nu$$

so that $v_\mathcal{S}$ is orthogonal to ν and tangential to all level surfaces of Φ. By a dot we denote the material derivative of a scalar

function $\eta = \eta(x,t)$ defined on Γ_T:

$$\dot\eta = \frac{\partial \eta}{\partial t} + v \cdot \nabla \eta. \tag{2.7}$$

In particular we note that $\dot\eta$ restricted to a given level surface

$$\Gamma_r := \{(x,t) : x \in \Gamma, t \in (0,T), \Phi(x,t) = r\}$$

depends only on the values of η on that level surface in space-time.

It is convenient to note that

$$\begin{aligned}\nabla_\Phi \cdot v &= \nabla_\Phi \cdot (Vv) + \nabla_\Phi \cdot v_\mathcal{S} \\ &= V \nabla_\Phi \cdot \nu + \nabla_\Phi \cdot v_\mathcal{S} = -V H_\Phi + \nabla_\Phi \cdot v_\mathcal{S}\end{aligned} \tag{2.8}$$

and

$$\nabla_\Phi \cdot v = \operatorname{trace}\left((\mathcal{P}_\Phi \nabla v\right).$$

For a scalar η we have

$$v \cdot \nabla \eta = V \nu \cdot \nabla \eta + v_\mathcal{S} \cdot \nabla \eta. \tag{2.9}$$

Lemma 3 (Implicit surface Leibniz formula) *Let Φ be a level set function and η be an arbitrary function defined on Γ_T such that the following quantities exist. Then*

$$\frac{d}{dt}\int_\Gamma \eta |\nabla \Phi| = \int_\Gamma \left(\dot\eta + \eta \nabla_\Phi \cdot v\right) |\nabla \Phi| - \int_{\partial\Gamma} \eta\, v \cdot \nu_{\partial\Gamma} |\nabla \Phi|. \tag{2.10}$$

Proof Noting that $\partial_t |\nabla \Phi| = \nu \cdot \nabla \Phi_t$ straightforward calculation yields

$$\frac{d}{dt}\int_\Gamma \eta |\nabla \Phi| = \int_\Gamma \left(\eta_t |\nabla \Phi| + \eta \nu \cdot \nabla \Phi_t\right).$$

Integration by parts on the second term in the integrand gives

$$\begin{aligned}\frac{d}{dt}\int_\Gamma \eta |\nabla \Phi| = \int_\Gamma |\nabla \Phi| \left(\eta_t + V \nabla \eta \cdot \nu - \eta v \cdot \nu H_\Phi\right) \\ - \int_{\partial\Gamma} \eta \nu \cdot \nu_{\partial\Gamma} V |\nabla \Phi|.\end{aligned}$$

The Eulerian divergence theorem (2.5) gives

$$\begin{aligned}-\int_\Gamma \eta v \cdot \nu H_\Phi |\nabla \Phi| = \int_\Gamma \nabla_\Phi \cdot (\eta v) |\nabla \Phi| \\ - \int_{\partial\Gamma} \eta v \cdot (\nu_{\partial\Gamma} - \nu \cdot \nu_{\partial\Gamma} \nu) |\nabla \Phi|\end{aligned}$$

and observing that

$$V \nabla \eta \cdot \nu + \nabla_\Phi \cdot (\eta v) = v \cdot \nabla \eta + \eta \nabla_\Phi \cdot v$$

yields the desired result. □

3 Conservation and diffusion

3.1 Eulerian conservation and diffusion

Let $\Phi : \Gamma_T \to \mathbb{R}$ be a prescribed non-degenerate level set function. Let $Q : \Gamma_T \to \mathbb{R}^{n+1}$ be a given flux. Then the Eulerian conservation law we consider is

$$\frac{d}{dt}\int_R u |\nabla \Phi| = -\int_{\partial R} (Q + |\nabla \Phi| u v) \cdot \nu_{\partial R} \tag{3.1}$$

for each sub-domain R of Γ where $\nu_{\partial R}$ is the outward unit normal to ∂R. In particular we consider a flux of the form

$$Q = |\nabla \Phi| q_\Phi$$

where $q_\Phi : \Gamma_T \to \mathbb{R}^{n+1}$ is a flux satisfying

$$q_\Phi \cdot \nu = 0. \tag{3.2}$$

It follows by the implicit surface Leibniz formula (2.10) that

$$\begin{aligned}\frac{d}{dt}\int_R u |\nabla \Phi| = \int_R \left(\dot u + u \nabla_\Phi \cdot v\right) |\nabla \Phi| \\ - \int_{\partial R} u v \cdot \nu_{\partial R} |\nabla \Phi|\end{aligned} \tag{3.3}$$

and by Eulerian integration by parts and (3.2) that

$$\int_{\partial R} q_\Phi \cdot \nu_{\partial R} |\nabla \Phi| = \int_R \nabla_\Phi \cdot q_\Phi |\nabla \Phi|. \tag{3.4}$$

It follows that

$$\int_R |\nabla \Phi| (\dot u + u \nabla_\Phi \cdot v + \nabla_\Phi \cdot q_\Phi) = 0$$

for every sub-domain R which implies the partial differential equation

$$\dot u + u \nabla_\Phi \cdot v + \nabla_\Phi \cdot q_\Phi = 0 \quad \text{in } \Gamma. \tag{3.5}$$

Taking q_Φ to be the diffusive flux

$$q_\Phi = -\mathcal{A} \nabla_\Phi u \tag{3.6}$$

leads to the diffusion equation

$$\dot u + u \nabla_\Phi \cdot v - \nabla_\Phi \cdot (\mathcal{A} \nabla_\Phi u) = 0. \tag{3.7}$$

Here $\mathcal{A} \geq 0$ is a symmetric mobility tensor with the property that it maps the tangent space

$$\mathcal{T} = \{\nu^\perp \in \mathbb{R}^{n+1} : \nu \cdot \nu^\perp = 0\}$$

into itself, so that

$$\mathcal{A} \nu^\perp \cdot \nu = 0 \; \forall \nu^\perp \in \mathcal{T}.$$

Observe that (3.7) is a linear degenerate parabolic equation because $\mathcal{P}_\Phi$ has a zero eigenvalue in the normal direction ν.

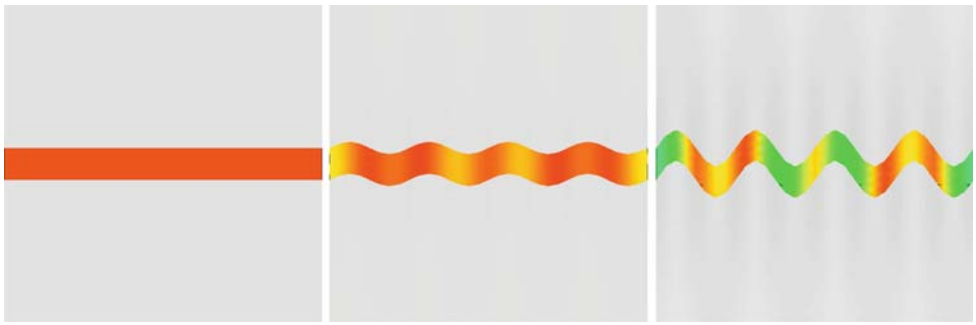

Fig. 1 Heating by motion: Solution of Example 5 for the times $t = 0.0, 0.039$ and 0.12 on the strip Ω_δ

Another form of this PDE, less suitable for numerical purposes than (3.7) is given as

$$u_t + V\frac{\partial u}{\partial \nu} + \nabla_\Phi \cdot (u v_S) - V H_\Phi u - \nabla_\Phi \cdot (\mathcal{A}\nabla_\Phi u) = 0.$$

In Fig. 1 we show an example for the influence of motion of the levels of Φ onto the solution u. We use $\Omega = (-1, 1)^2 \subset \mathbb{R}^2$ and a level set function Φ [see (6.5)] which deforms straight lines in Ω into curved lines. Constant initial data $u_0 = 1$ then become nonconstant during the evolution. In Fig. 1 we show a strip cut out of the computational domain. For a detailed description we refer to Example 5.

The variational form of (3.7) is obtained in the following way. For each level surface of Φ we multiply Eq. (3.7) by a test function η and get

$$\int_\Omega (\dot{u} + u\nabla_\Phi \cdot v - \nabla_\Phi \cdot (\mathcal{A}\nabla_\Phi u))\, \eta |\nabla\Phi| = 0.$$

Observe that the Leibniz formula, (2.10), gives

$$\frac{d}{dt}\int_\Omega u\eta|\nabla\Phi| = \int_\Omega (\dot{u} + u\nabla_\Phi \cdot v)\, \eta|\nabla\Phi| + \int_\Omega u\dot{\eta}|\nabla\Phi| - \int_{\partial\Omega} u\eta v \cdot \nu_{\partial\Omega}|\nabla\Phi|,$$

and because of $\mathcal{A}\nabla_\Phi u \cdot \nu = 0$ integration by parts (2.6) gives

$$\int_\Omega \mathcal{A}\nabla_\Phi u \cdot \nabla_\Phi \eta |\nabla\Phi| = -\int_\Omega \eta \nabla_\Phi \cdot (\mathcal{A}\nabla_\Phi u)\, |\nabla\Phi| + \int_{\partial\Omega} \mathcal{A}\nabla_\Phi u \cdot \nu_{\partial\Omega}\eta|\nabla\Phi|.$$

In order to proceed we need a boundary condition for u on $\partial\Omega$. For the purpose of this paper, we shall assume that

$$v \cdot \nu_{\partial\Omega} = 0 \text{ on } \partial\Omega \tag{3.8}$$

and impose the zero flux condition

$$|\nabla\Phi|\mathcal{A}\nabla_\Phi u \cdot \nu_{\partial\Omega} = 0 \ \text{ on } \ \partial\Omega. \tag{3.9}$$

Finally, we obtain

$$\frac{d}{dt}\int_\Omega u\eta|\nabla\Phi| + \int_\Omega \mathcal{A}\nabla_\Phi u \cdot \nabla_\Phi \eta|\nabla\Phi| = \int_\Omega u\dot{\eta}|\nabla\Phi|. \tag{3.10}$$

Remark 3 Taking $\eta = 1$ we find the conservation equation

$$\frac{d}{dt}\int_\Omega u|\nabla\Phi| = 0.$$

4 Weak form and energy estimate

We introduce the notion of a weak solution of the linear degenerate Eulerian parabolic (3.7), for which we derived a variational form in (3.10). We define the normed linear spaces

$$L^2_\Phi(\Omega_T) = \{\eta : \langle\eta, \eta\rangle_\Phi < \infty\},$$
$$H^1_\Phi(\Omega_T) = \{\eta : \eta, \dot{\eta}, \nabla_\Phi\eta \in L^2_\Phi(\Omega_T)\},$$

where the norm is induced by the inner product

$$\langle\eta, \xi\rangle_\Phi = \int_0^T\int_\Omega \eta\xi|\nabla\Phi|,$$
$$\langle\eta, \xi\rangle_{H^1_\Phi} = \langle\eta, \xi\rangle_\Phi + \langle\dot{\eta}, \dot{\xi}\rangle_\Phi + \langle\nabla_\Phi\eta, \nabla_\Phi\xi\rangle_\Phi,$$

and we set

$$||\eta||_{L^2_\Phi(\Omega_T)} = \sqrt{\langle\eta, \eta\rangle_\Phi},$$
$$||\eta||_{H^1_\Phi(\Omega_T)} = \sqrt{\langle\eta, \eta\rangle_{H^1_\Phi}}.$$

Definition 1 (Weak solution) A function $u \in H^1_\Phi(\Omega_T)$ is a weak solution of (3.7) and (3.9), if for almost every $t \in (0, T)$

$$\frac{d}{dt}\int_\Omega u\eta|\nabla\Phi| + \int_\Omega \mathcal{A}\nabla_\Phi u \cdot \nabla_\Phi\eta|\nabla\Phi| = \int_\Omega u\dot{\eta}|\nabla\Phi| \tag{4.1}$$

for every $\eta \in H^1_\Phi(\Omega_T)$.

Weak solutions satisfy the following basic energy estimate whose discrete counterpart implies stability. Throughout we will assume the initial condition

$$u(\cdot, 0) = u_0(\cdot) \quad \text{on } \Omega. \tag{4.2}$$

Lemma 4 *Let u satisfy (4.1). Then*

$$\frac{1}{2}\frac{d}{dt}\int_\Omega u^2|\nabla\Phi| + \int_\Omega \mathcal{A}\nabla_\Phi u\cdot\nabla_\Phi u|\nabla\Phi| + \frac{1}{2}\int_\Omega u^2\,\nabla_\Phi\cdot v|\nabla\Phi| = 0. \tag{4.3}$$

Proof We choose $\eta = u$ in (4.1) and obtain

$$\begin{aligned}
&\frac{d}{dt}\int_\Omega u^2|\nabla\Phi| + \int_\Omega \mathcal{A}\nabla_\Phi u\cdot\nabla_\Phi u|\nabla\Phi| \\
&= \int_\Omega u\dot u|\nabla\Phi| \\
&= \frac{1}{2}\int_\Phi \left(u^2\right)^\cdot|\nabla\Phi| \\
&= \frac{1}{2}\frac{d}{dt}\int_\Omega u^2|\nabla\Phi| - \frac{1}{2}\int_\Omega u^2\,\nabla_\Phi\cdot v|\nabla\Phi| \\
&\quad + \frac{1}{2}\int_{\partial\Omega} u^2 v\cdot\nu_{\partial\Omega}|\nabla\Phi|,
\end{aligned}$$

where the last term vanishes because of (3.8), and this was the claim. □

5 Finite element approximation

5.1 Semi-discrete approximation

Our Eulerian ESFEM is based on the the weak form (4.1) of the diffusion equation. We use fixed in time finite element functions so that the test functions now will satisfy

$$\dot\eta = v\cdot\nabla\eta.$$

We assume that the domain Ω is triangulated by an admissible triangulation $\mathcal{T}_h = \cup_{T\in\mathcal{T}_h} T$ which consists of simplices T. The discrete space then is

$$S_h = \{U\in C^0(\overline{\Omega}) | U|_T \text{ is a linear polynomial, } T\in\mathcal{T}_h\}.$$

The discrete space is generated by the nodal basis functions $\chi_i, i = 1,\dots,N$,

$$S_h = \operatorname{span}\{\chi_1,\dots,\chi_N\}.$$

It is possible to generalize the method to higher order finite elements.

Definition 2 (Semi-discretization in space) Find $U(\cdot,t)\in S_h$ such that

$$\frac{d}{dt}\int_\Omega U\eta|\nabla\Phi| + \int_\Omega \mathcal{A}\nabla_\Phi U\cdot\nabla_\Phi\eta|\nabla\Phi| = \int_\Omega Uv\cdot\nabla\eta|\nabla\Phi| \quad \forall\eta\in S_h. \tag{5.1}$$

Using the Leibniz formula it is easily seen that an equivalent formulation is:

$$\int_\Omega \dot U\eta|\nabla\Phi| + \int_\Omega U\eta\nabla_\Phi\cdot v|\nabla\Phi| + \int_\Omega \mathcal{A}\nabla_\Phi U\cdot\nabla_\Phi\eta|\nabla\Phi| = 0 \quad \forall\eta\in S_h.$$

Setting

$$U(\cdot,t) = \sum_{j=1}^N \alpha_j(t)\chi_j(\cdot,t)$$

we find that

$$\frac{d}{dt}\left(\int_\Omega \sum_{j=1}^N \alpha_j\chi_j\eta|\nabla\Phi|\right) + \int_\Omega \mathcal{A}\sum_{j=1}^N \alpha_j\nabla_\Phi\chi_j\cdot\nabla_\Phi\eta|\nabla\Phi| = \int_\Omega \sum_{j=1}^N \alpha_j\chi_j v\cdot\nabla\eta|\nabla\Phi|$$

forall $\eta\in S_h$ and taking $\eta = \chi_k$, $k = 1,\dots,N$, we obtain

$$\frac{d}{dt}\left(\mathcal{M}(t)\alpha\right) + \mathcal{S}(t)\alpha = \mathcal{C}(t)\alpha \tag{5.2}$$

where $\mathcal{M}(t)$ is the evolving mass matrix

$$\mathcal{M}(t)_{kj} = \int_\Omega \chi_j\chi_k|\nabla\Phi|,$$

$\mathcal{C}(t)$ is a transport matrix

$$\mathcal{C}(t)_{kj} = \int_\Omega \chi_j v\cdot\nabla\chi_k|\nabla\Phi|,$$

and $\mathcal{S}(t)$ is the evolving stiffness matrix

$$\mathcal{S}(t)_{jk} = \int_\Omega \mathcal{A}\nabla_\Phi\chi_j\nabla_\Phi\chi_k|\nabla\Phi|.$$

Since the mass matrix $\mathcal{M}(t)$ is uniformly positive definite on $[0,T]$ and the other matrices are bounded, we get existence and uniqueness of the semi-discrete finite element solution.

Remark 4 A significant feature of our approach is the fact that the matrices $\mathcal{M}(t)$, $\mathcal{C}(t)$ and $\mathcal{S}(t)$ depend only on the evaluation of the gradient of the level set function Φ and the velocity field v. The method does not require a numerical evaluation of the curvature.

5.2 Stability

The basic stability result for our spatially discrete scheme from Definition 2 is given in the following Lemma.

Lemma 5 (Stability) *Let U be a solution of the semi-discrete scheme as in Definition 2 with initial value $U(\cdot,0)=U_0$.*

Assume that

$$\int_0^T \|\nabla_\Phi \cdot v\|_{L^\infty(\Omega)} < \infty$$

and that

$$\mathcal{A}\xi\cdot\xi \geq a_0|\xi|^2$$

with some $a_0>0$ for every $\xi\in\mathbb{R}^{n+1}$ with $\xi\cdot\nu=0$.

Then the following stability estimate holds:

$$\sup_{(0,T)} \|U\|^2_{L^2_\Phi(\Omega)} + \int_0^T \|\nabla_\Phi U\|^2_{L^2_\Phi(\Omega)} \leq c\|U_0\|^2_{L^2_\Phi(\Omega)}\,. \quad (5.3)$$

Proof The estimate follows from the Leibniz formula in Lemma 3 in the same way as this was done for the continuous equation in Lemma 4 and a standard Gronwall argument. □

6 Implementation and numerical results

6.1 Implicit Euler scheme

The time discretization in our computations is done by an implicit method. We discretize the variational form (3.10) in time. The spatially discrete problem is

$$\frac{d}{dt}\int_\Omega U\eta|\nabla\Phi| + \int_\Omega \mathcal{A}\nabla_\Phi U\cdot\nabla_\Phi\eta|\nabla\Phi| = \int_{\Gamma_h(t)} U\dot\eta|\nabla\Phi| \quad \forall\eta\in S_h. \quad (6.1)$$

We introduce a time step size $\tau>0$ and use upper indices for the time levels. Thus U^m represents $U(\cdot,m\tau)$. With these notations we propose the following Algorithm.

Algorithm 1 (Fully discrete scheme) Let $U^0\in S_h$ be given. For $m=0,\dots,m_T$ solve the linear system

$$\frac{1}{\tau}\int_\Omega U^{m+1}\eta|\nabla\Phi^{m+1}| + \int_\Omega \mathcal{A}^{m+1}\nabla_{\Phi^{m+1}}U^{m+1}\cdot\nabla_{\Phi^{m+1}}\eta|\nabla\Phi^{m+1}| = \frac{1}{\tau}\int_\Omega U^m\eta|\nabla\Phi^m| + \int_\Omega U^m v^m\cdot\nabla\eta|\nabla\Phi^m| \quad (6.2)$$

for all $\eta\in S_h$.

The transport term on the right-hand side of (6.2) is treated explicitly. Depending on the velocity v of the levels it may be necessary to employ techniques for diffusion convection equations.

6.2 Numerical tests

Example 1 To start with we solve the heat equation on a moving circle. We choose Ω to be the annular region with outer radius 1 and inner radius 0.5. We set

$$\Phi(x,t) = |x| - 0.75 + \sin(4t)\,(|x|-0.5)\,(1-|x|)$$

so that the boundary $\partial\Omega$ comprises level lines of Φ. The velocity v is chosen to be normal, $v_S=0$. The function $u(x,t)=\exp(-t/|x|^2)x_1/|x|$ then solves

$$\dot u + u\nabla_\Phi\cdot v - \Delta_\Phi u = f$$

where we calculate $f=Vu\left(\frac{2t}{r^3}+\frac{1}{r}\right)$ from

$$f = u_t + V\frac{\partial u}{\partial r} - uVH - \frac{1}{r^2}u_{\theta\theta}$$

where $x=r(\cos\theta,\sin\theta)$. We are interested in u on the moving curve

$$\Gamma(t) = \left\{x\in\Omega\,|\,\Phi(x,t)=\frac{3}{4}\right\}.$$

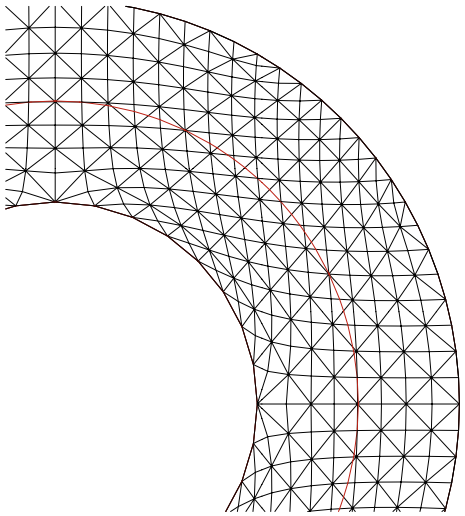

Fig. 2 Example 1: Triangulation of Ω (*black*) and Curve Γ (*red*) for a quarter of the annulus

Table 1 Heat equation on an evolving curve

h	$L^\infty(L^2_\Phi(\Omega))$	eoc	$L^2(H^1_\Phi(\Omega))$	eoc
0.5176	0.1219	–	0.1742	–
0.2805	0.08354	0.61	0.07678	1.33
0.1563	0.02914	1.80	0.02846	1.69
0.08570	0.009000	1.95	0.01095	1.58
0.04657	0.002681	1.98	0.004598	1.42
0.02492	0.0007709	1.99	0.002077	1.27

Errors and experimental orders of convergence in Φ-norms for Example 1 on Ω

Table 2 The same situation as in Table 1

h	$L^\infty(L^2(\Omega))$	eoc	$L^2(H^1(\Omega))$	eoc
0.5176	0.1210	–	0.6770	–
0.2805	0.08648	0.54	0.4779	0.56
0.1563	0.02939	1.84	0.2151	1.36
0.08570	0.009019	1.96	0.1166	1.01
0.04657	0.002682	1.98	0.06947	0.84
0.02492	0.0007887	1.95	0.04427	0.72

Errors and experimental orders of convergence in the full $L^2(\Omega)$-norms

Table 3 The same situation as in Table 1

h	$L^\infty(L^2(\Gamma))$	eoc	$L^2(H^1(\Gamma))$	eoc
0.5176	0.1205	–	0.1803	–
0.2805	0.04464	1.62	0.08060	1.31
0.1563	0.01241	2.18	0.02807	1.80
0.08570	0.003408	2.14	0.01189	1.42
0.04657	0.0008736	2.23	0.005745	1.19
0.02492	0.0002445	2.03	0.002863	1.11

Errors and experimental orders of convergence on Γ

Table 4 Maximum errors on Ω and on Γ for the situation of Example 1

h	$L^\infty(L^\infty(\Omega))$	eoc	$L^\infty(L^\infty(\Gamma))$	eoc
0.5176	0.2123	–	0.09084	–
0.2805	0.1712	0.35	0.03752	1.44
0.1563	0.06420	1.67	0.008879	2.46
0.08570	0.02667	1.46	0.002789	1.92
0.04657	0.01184	1.33	0.0007421	2.17
0.02492	0.005510	1.22	0.0001975	2.11

As initial data we take $u_0(x) = x_1/|x|$. We have chosen the coupling $\tau = h^2$ in order to show the higher order convergence for L^2 and L^∞ errors. The time interval is $T = 1.0$. In Fig. 2 we show part of the used grid with the curve $\Gamma(0)$ cutting the triangulation. In Table 1 we show the absolute errors and the corresponding experimental orders of convergence for the Φ-norms on the full domain Ω, abbreviated by

$$L^\infty(L^2_\Phi(\Omega)) = \sup_{(0,T)} \|u - u_h\|_{L^2_\Phi(\Omega)},$$

$$L^2(H^1_\Phi(\Omega)) = \left(\int_0^T \|\nabla_\Phi (u - u_h)\|^2_{L^2_\Phi(\Omega)} \right)^{\frac{1}{2}}.$$

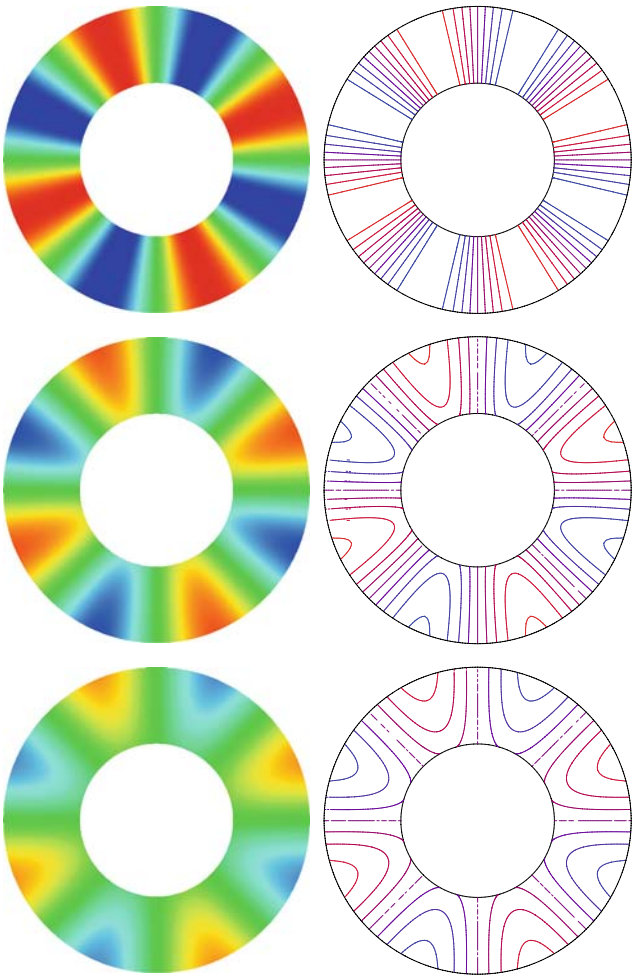

Fig. 3 Solution u of Example 2 for the times $t = 0.0$, $t = 0.011$ and $t = 0.023$. The colour red stands for $u = 1$ and the colour blue for $u = -1$. Left column shows the solution on Ω in this colour code, right column: the levels

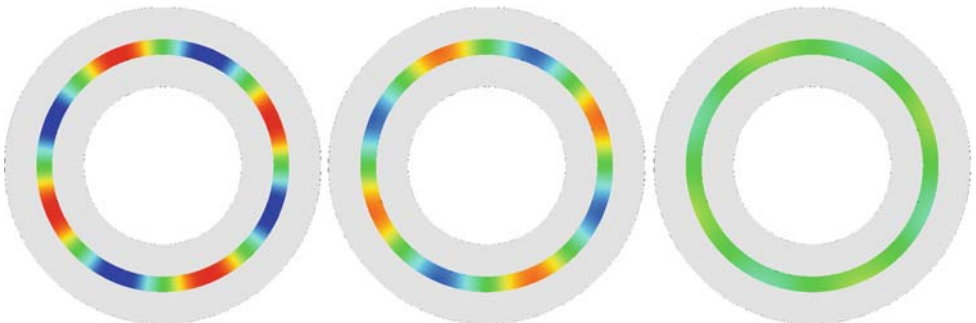

Fig. 4 Solution u of Example 2 for the times $t = 0.0$, $t = 0.01$ and $t = 0.05$ on the strip $0.7 < |x| < 0.8$. The colouring is the same as in Fig. 3

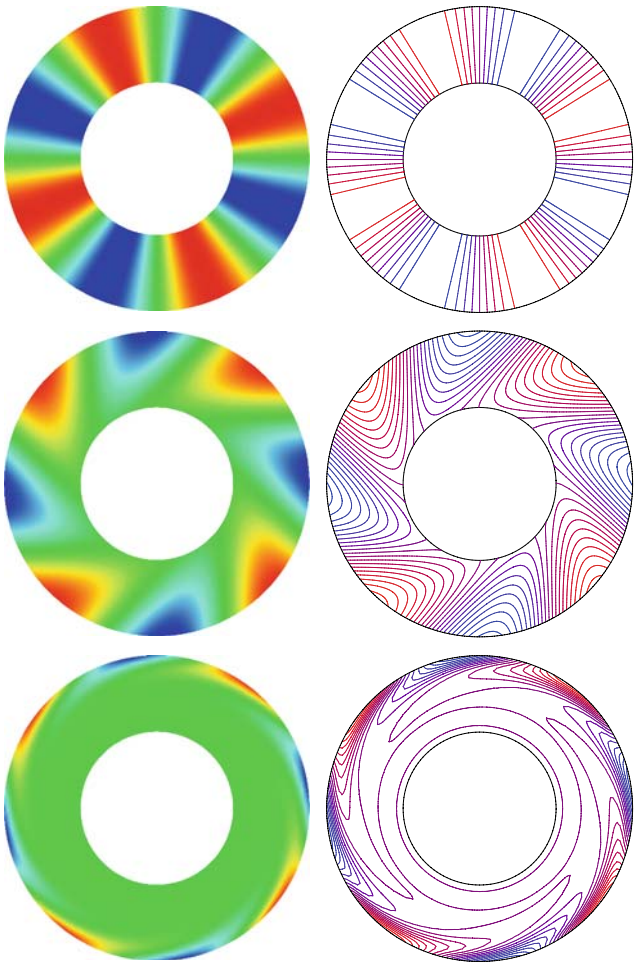

Fig. 5 Solution u of Example 3 with tangential velocity (6.3) for the times $t = 0.0$, $t = 0.046$ and $t = 0.37$. The colour stands for the values of u between maximum (*red*) and minimum (*blue*)

For comparison we show in Table 2 the usual $L^2(\Omega)$-norms for the error,

$$L^\infty(L^2(\Omega)) = \sup_{(0,T)} \|u - u_h\|_{L^2(\Omega)},$$

$$L^2(H^1(\Omega)) = \left(\int_0^T \|\nabla(u - u_h)\|^2_{L^2(\Omega)} \right)^{\frac{1}{2}}.$$

The most important errors are shown in Table 3. Here, we show the asymptotic order of the adequate norms on the curve $\Gamma(t)$,

$$L^\infty(L^2(\Gamma)) = \sup_{(0,T)} \|u - u_h\|_{L^2(\Gamma)},$$

$$L^2(H^1(\Gamma)) = \left(\int_0^T \|\nabla_\Phi(u - u_h)\|^2_{L^2(\Gamma)} \right)^{\frac{1}{2}}.$$

We observe that despite the quite irregular discretization of the curves induced by the triangulation of Ω the orders are two for the $L^\infty(L^2(\Gamma))$-norm and one for the $L^2(H^1(\Gamma))$-norm.

As an additional information we show the maximum norms

$$L^\infty(L^\infty(\Omega)) = \sup_{(0,T)} \|u - u_h\|_{L^\infty(\Omega)},$$

$$L^\infty(L^\infty(\Gamma)) = \sup_{(0,T)} \|u - u_h\|_{L^2(\Gamma)}$$

on Ω and Γ in Table 4.

For an error $E(h_1)$ and $E(h_2)$ for the grid sizes h_1 and h_2 the experimental order of convergence is defined as

$$\mathrm{eoc}(h_1, h_2) = \log \frac{E(h_1)}{E(h_2)} \left(\log \frac{h_1}{h_2} \right)^{-1}.$$

Example 2 We solve the Φ-heat equation on concentric circles. We start with the stationary situation, i.e. $\Phi_t = 0$. We take

$$\Omega = \left\{ x \in \mathbb{R}^2 \,|\, \frac{1}{2} < |x| < 1 \right\},$$

$u_0(x) = \sin(4\varphi)$ and

$\Phi(x, t) = |x| - 0.75$

together with $v_S = 0$. Since the mean value of u_0 on concentric circles vanishes, the solution tends to zero as time tends to infinity. But this occurs at a rate which depends on the radius of the circle because of the different diffusion coefficients on the different circles. This effect is shown in Fig. 3 for small times. In this computation we used the time step $\tau = 10^{-5}$ and spatial grid size $h = 0.03026$. In Fig. 4 we additionally show the solution on a strip cut out of the domain by the level set function Φ.

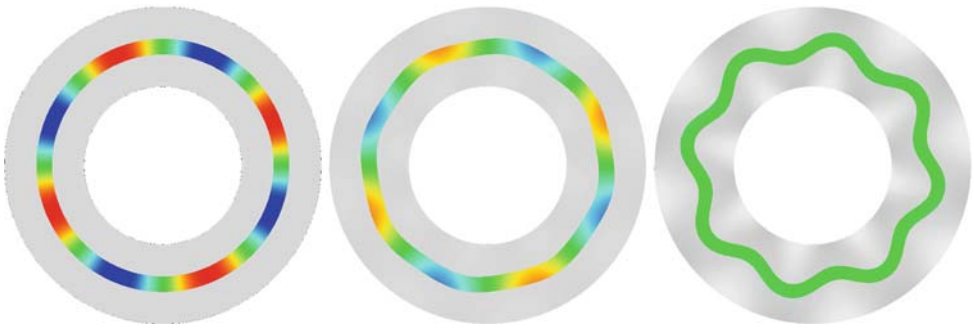

Fig. 6 Solution u of Example 4 with normal velocity induced by (6.4) for the time steps 0,100 and 1,000. The colour stands for the values of u between maximum (*red*) and minimum (*blue*) on Ω

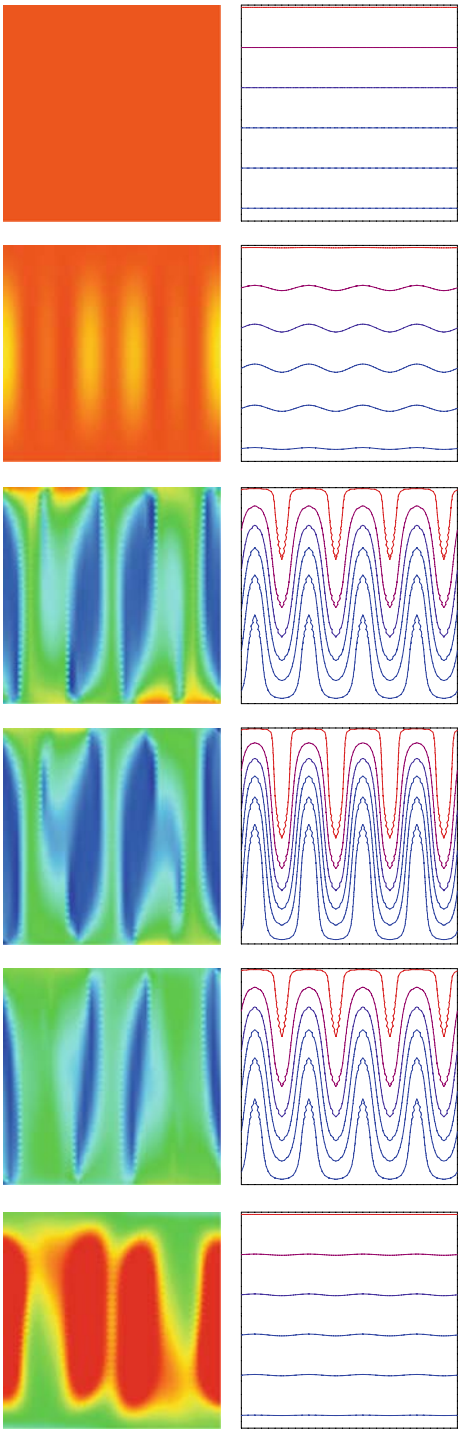

Fig. 7 Solution (*left*) of Example 5 with levels of Φ (*right*) for the times $t = 0.0, 0.039, 0.426, 0.813, 2.36$ and 3.13 and Blue represents the value $u = -0.1$ and red $u = 1.1$

Example 3 We next compute the solution for a similar situation as above but now with purely tangential velocity

$$v_S = 10\frac{(-\Phi_{x_2}, \Phi_{x_1})}{|\nabla\Phi|}. \tag{6.3}$$

In Fig. 5 we show the solution at some time steps.

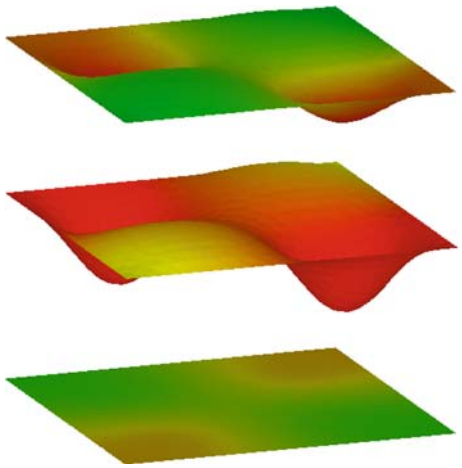

Fig. 8 Example 6: Values of the solution u for the times $0.47, 0.94$ and 2.0 on the surface $\Phi = 0.75$

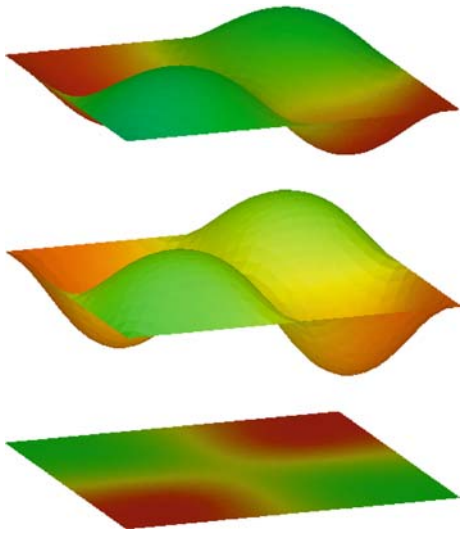

Fig. 9 Example 6: Values of the solution u for the times $0.47, 0.94$ and 2.0 on the surface $\Phi = 0.25$

Example 4 Finally, we compute the evolution with purely normal velocity. For this we have chosen

$$\Phi((r\cos\theta, r\sin\theta), t) = r - 0.75 + \sin(8\theta)\sin(4t)(r - 0.5)(1 - r). \tag{6.4}$$

In Fig. 6 we show some time steps. In order to identify the zero level set of Φ, on which we want to solve the PDE, we show a strip of width 0.05 around that zero level set. The colouring is as in the previous examples. The colours range from minimum to maximum of u on Ω.

Example 5 We choose $\Omega = (-1, 1)^2$ and constant initial data

$$u_0(x_1, x_2) = 1.$$

The level set function is given by

$$\Phi(x_1, x_2, t) = x_2 - (1 - x_2^2)\sin(4\pi x_1)\sin(t), \tag{6.5}$$

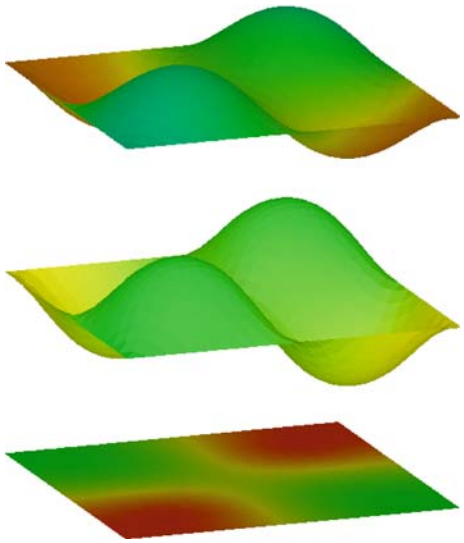

Fig. 10 Example 6: Values of the solution u for the times 0.47, 0.94 and 2.0 on the surface $\Phi = 0.0$

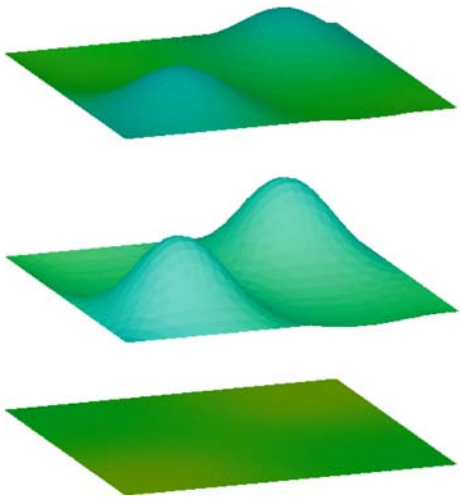

Fig. 11 Example 6: Values of the solution u for the times 0.47, 0.94 and 2.0 on the surface $\Phi = -0.75$

and we use $\tau = 0.000390625$ and $h = 0.0625$. In Fig. 7 we show the solution for times from one period of the level set function Φ. The time dependent levels of Φ are shown in the same Figure. In Fig. 1 we have shown the solution on the strip

$$\Omega_\delta = \{x \in \Omega \,|\, |\Phi(x,t)| < \delta\}$$

for $\delta = 0.1$ for some time steps to demonstrate the effect of "heating by motion".

Example 6 We finish with a three dimensional example. We apply our numerical method to the domain $\Omega = (-1,1)^3 \subset \mathbb{R}^3$ and to the surfaces which are implicitly given by the function

$$\Phi(x,t) = x_3 - \frac{1}{2}(1 - x_3^2)\sin(\pi x_1)\sin(\pi x_2)\sin\left(\frac{\pi}{2}t\right). \tag{6.6}$$

As initial value we have chosen the constant function $u_0 = 1$. In Figs. 8, 9, 10 and 11 we show the results of the computation for some time steps. The colouring of the surfaces is given by the values of the solution u. Here, dark blue represents $u = 0.0$, red $u = 2.0$ and the colours are linearly interpolated. Green represents the value $u = 1.0$. The computational data were $N = 35937$ and $\tau = 0.0003125$.

Acknowledgments The work was supported by the Deutsche Forschungsgemeinschaft via DFG-Forschergruppe *Nonlinear partial differential equations: Theoretical and numerical analysis* and by the UK EPSRC via the Mathematics Research Network: *Computation and Numerical analysis for Multiscale and Multiphysics Modelling*. Part of this work was done during a stay of the first author at the ICM at the University of Warsaw supported by the *Alexander von Humboldt Honorary Fellowship 2005* granted by the Foundation for Polish Science.

The graphical presentations were performed with the package GRAPE. The three dimensional computations have been done with the finite element package ALBERTA [20]. For technical help we thank C. Eilks, C.-J. Heine, M. Lenz and R. Klöfkorn.

References

1. Dziuk, G., Elliott, C.M.: Finite elements on evolving surfaces. IMA J. Numer. Anal. **27**, 262–292 (2007)
2. Dziuk, G., Elliott, C.M.: Surface finite elements for parabolic equations. J. Comp. Math. **25**, 385–407 (2007)
3. Dziuk, G., Elliott, C.M.: Eulerian finite element method for parabolic PDEs on implicit surfaces. Interfaces Free Boundaries **10** (2008)
4. Deckelnick, K., Dziuk, G., Elliott, C.M., Heine, C.-J.: An h-narrow band finite element method for elliptic equations on implicit surfaces (in preparation)
5. Bertalmio, M., Memoli, F., Cheng, L.T., Osher, S., Sapiro, G.: Variational problems and partial differential equations on implicit surfaces:bye bye triangulated surfaces? Geometric level set methods in imaging, vision and graphics Springer New York, pp 381–397 (2003)
6. Bertalmio, M., Cheng, L.T., Osher, S., Sapiro, G.: Variational problems and partial differential equations on implicit surfaces. J. Comp. Phys. **174**, 759–780 (2001)
7. Greer, J.B.: An improvement of a recent Eulerian method for solving PDEs on general geometries. J. Sci. Comput. **29**, 321–352 (2006)
8. Greer, J., Bertozzi, A., Sapiro, G.: Fourth order partial differential equations on general geometries. J. Comput. Phys. **216**(1), 216–246 (2006)
9. Burger, M.: Finite element approximation of elliptic partial differential equations on implicit surfaces. Comput. Visual. Sci. (2007). doi:10.1007/s00791-007-0081-x
10. Adalsteinsson, D., Sethian, J.A.: Transport and diffusion of material quantities on propagating interfaces via level set methods. J. Comp. Phys. **185**, 271–288 (2003)
11. Xu, J.-J., Zhao, H.-K.: An Eulerian formulation for solving partial differential equations along a moving interface. J. Sci. Comput. **19**, 573–594 (2003)

12. James, A.J., Lowengrub, J.: A surfactant-conserving volume-of-fluid method for interfacial flows with insoluble surfactant. J. Comp. Phys. **201**, 685–722 (2004)
13. Stone, H.A.: A simple derivation of the time-dependent convective-diffusion equation for surfactant transport along a deforming interface. Phys. Fluids A **2**, 111–112 (1990)
14. Cahn, J.W., Fife, P., Penrose, O.: A phase field model for diffusion induced grain boundary motion. Acta Mater. **45**, 4397–4413 (1997)
15. Deckelnick, K., Elliott, C.M., Styles, V.: Numerical diffusion induced grain boundary motion. Interfaces Free Boundaries **3**, 393–414 (2001)
16. Fife, P., Cahn, J.W., Elliott, C.M.: A free boundary model for diffusion induced grain boundary motion. Interfaces Free Boundaries **3**, 291–336 (2001)
17. Mayer, U.F., Simonnett, G.: Classical solutions for diffusion induced grain boundary motion. J. Math. Anal. **234**, 660–674 (1999)
18. Leung, C.H., Berzins, M.: A computational model for organism growth based on surface mesh generation. J. Comp. Phys. **188**, 75–99 (2003)
19. Jin, H., Yezzi, A.J., Soatto, S.: Region based segmentation on evolving surfaces with application to 3D reconstruction of shape and piecewise constant radiance. UCLA Preprint (2004)
20. Schmidt, A., Siebert, K.G.: Design of adaptive finite element software. The finite element toolbox ALBERTA. Springer Lecture Notes in Computational Science and Engineering, vol. 42. Springer, Berlin (2004)